UNIVERSITY OF TARTU
FACULTY OF SCIENCE AND TECHNOLOGY
INSTITUTE OF TECHNOLOGY

Selin Su Yegit

Synthesis of zirconium carbide derived carbon using sol-gel method, carbothermal reduction and chlorination

Bachelor's thesis (12 ECTs)

Supervisor: PhD Maarja Paalo

Tartu 2022

Table of Contents

1. Introduction **6**
2. Literature overview **8**
2.1 Carbides 8
2.1.1 Interstitial carbides and transition metals 9
2.2 Sol gel method 10
2.2.1 Sol-gel method for metal alkoxides 11
2.3 Carbide derived carbon 12
2.3.1 Uses of carbide derived carbons 13
3. Experimental **15**
3.1 Synthesis of carbide derived carbons 15
3.1.1 Sol gel synthesis of zirconium carbide precursor 15
3.1.2 Pyrolysis, carbothermal reduction and chlorination 16
4. Results **18**
4.1 Precursor analysis 18
4.1.1 Molar ratio analysis 18
4.1.2 Infrared spectroscopy analysis of the precursor materials 19
4.2. Characterization of zirconium carbide materials 20
4.2.1. X-ray diffraction method 20
4.2.2 Sorption measurements data 21
4.2.3 Scanning electron microscopy 22
4.3. Characterization of zirconium carbide derived carbon materials 23
4.3.1 X-ray diffraction method 23
4.3.2 Raman spectroscopy 24
4.3.3 Sorption measurements data 25
4.3.4 Scanning electron microscopy 26
4.3.5 Transmission electron microscopy 27
5. Conclusions **29**
6. Summary **30**
7. Acknowledgements **31**
8. References **32**

ABBREVIATIONS

BET	Brunauer-Emmett-Teller
CDC	carbide derived carbon
IR	infrared spectroscopy
EDLC	electrical double-layer capacitor
M	metal group
NLDFT	non-local density functional theory
nm	nanometers
R	r group
SC	supercapacitor
S_{BET}	specific surface area calculated according to Brunauer-Emmett-Teller theory
S_{DFT}	specific surface area calculated according to density functional theory
SEM	scanning electron microscopy
TEM	transmission electron microscopy
TiC	titanium carbide
TiC-CDC	titanium carbide derived carbon
V_{DFT}	volume of pores calculated according to density functional theory
V_{tot}	total volume of pores
ZrC	zirconium carbide
ZrC-CDC	zirconium carbide derived carbon
ZrO_2	zirconium oxide
XRD	X-ray diffraction
θ	phase angle between voltage and current

Synthesis of zirconium carbide derived carbon using sol-gel method, carbothermal reduction and chlorination

Abstract:

The synthesis of zirconium carbide (ZrC) was carried out using sol-gel method, pyrolysis, carbothermal reduction, and chlorination of the ZrC to obtain the final carbon material (ZrC-CDC). The synthesis conditions are adjusted for the ideal environment, the obtained ZrC was compared to the commercial ZrC and showed to be much more amorphous while having oxide bonds. Still considering the slightly varying conditions for each sample the analysis data at hand show that the samples were relatively uniform in structure. The final carbon was obtained in 3 different ways by varying the chlorination temperature (700 °C, 800 °C, 900 °C) and was later characterized. The results at hand showed that the thermal treatments were successful at producing amorphous carbon at 800°C, with the lower and higher temperatures both still having oxide bonds. With the experiments done and analysis at hand it was found that the sol-gel synthesized ZrC-CDC could be an applicable candidate for applications in supercapacitors as an electrode material.

Keywords: ZrC, CDC, sol-gel method, micro- and mesoporous carbon

CERCS: T150 Material technology

Tsirkooniumkarbiidse süsiniku süntees sool-geeli meetodil, karbotermilise taandamise ja kloreerimise teel

Lühikokkuvõte:

Tsirkooniumkarbiidi (ZrC) süntees viidi läbi sool-geel meetodi abil, rakendades seejärel pürolüüsi, karbotermilist taandamistkõrgel temperatuuril, ja kloreerimist, saavutamaks soovitud karbiidset päritolud süsinik. Sünteesi tarbeks loodud tingimused kohandati ideaalilähedasteks. Katsejärgselt võrreldi sünteesitudtsirkooniumkarbiidi (ZrC) selle kommertsiaalse versiooniga: sünteesitud süsinik oli võrdluses amorfsem ning selle struktuuris esines oksiidvormi. Arvestades loodud tingimuste mõnetist kõikumist katsete kordamisel, näitavad saadud süsinike karakteriseerimise tulemused, et proovid on võrdlemisi ühtse struktuuriga. Lõplik süsinikuvorm saadi kolmel erineval viisil, varieerides kloreerimise temperatuuri (700 °C, 800 °C, 900 °C).

Käesolevad tulemused näitasid, et sool-geel meetodi kasutamine ja termiliste töötluste rakendamine amorfse süsinikuvormi saamiseks osutus edukaimaks 800 °C juures. Madalama ja kõrgema temperatuuriga töödeldud 5rove iseloomustas oksiidsidemete olemasolu. Tehtud katsed ja neil baseeruv analüüs näitasid, et sool-geel-meetodi abil sünteesitud ZrC-CDC-d oleks võimalik rakendada superkondensaatorites kui elektroodi materjali.

Võtmesõnad: ZrC, CDC, sool-geel meetod, mikro- ja mesopoorne süsinik

CERCS: T150 Materjalitehnoloogia

1. Introduction

The active change in technological advancements over the last decades has brought up a concern for our resources and a task for optimizing our energy storage given the damage that unsustainable energy sources have created. With the increasing economical struggle surrounding the energy crisis, better and cheaper energy storage mechanisms have become a priority with the industry focusing on supercapacitors in particular.

Supercapacitors today are known to bridge the gap between batteries and capacitors. H.I. Becker of General Electric was the first to patent an electrochemical capacitor device in 1957 but at the time it wasn't applicable as much due to the massive pool of electrolyte solution, it wasn't a practical or compact setup. With modern age as machines become smaller and more practical, the supercapacitor has also changed and become more applicable. Nowadays they are favored due to their fast-charging and discharging speed, long cycle life and high-power density, although the materials and electrolytes used for supercapacitors can be further optimized [1].

Supercapacitors use electrostatic ion adsorption on the electrolyte/electrode double-layer interfaces (for example of porous carbons with specific surface areas typically in the range of 1000 – 3000 $m^2 g^{-1}$) to store electrical energy [2]. The working principle of a supercapacitor is similar to a capacitor with the few differences being that the electrodes are closer and where there would be a dielectric substance between electrodes in a capacitor, the supercapacitor has an electrolyte solution, and the specific surface area of the electrodes is magnitudes higher. One of the proposed ways to advance supercapacitors has been to optimize the electrode material to increase both energy and power densities of the supercapacitors [3].

The electrode of a supercapacitor needs to have good conductivity, high-temperature stability, long term chemical-stability, high corrosion resistance and high surface areas. For the common application of supercapacitors, we would also want the material to be cheaper and lighter to be more applicable [4].

Studies have shown the synthesis and use of transition metal carbides as precursor materials for carbide derived carbons that are used as electrode materials in supercapacitors [5], [6]. Transition metal carbides have great electrical and thermal conductivity, high melting points, extremely high microhardness and resistance to nonoxidizing acids, making them a very attractive material to be put to use within the energy storage. They are traditionally synthesized by reaction of the elements at 2300 °C in hydrogen or an inert atmosphere. Different synthesis methods have

been shown in the literature including sputter deposition, chemical vapor deposition and even by sputter deposition [7].

The work at hand focuses on the use of sol-gel method for the synthesis of zirconium carbide (ZrC). Sol-gel method is preferred since it lowers the carbothermal reduction temperature and needed time due to the smaller diffusion distance. It also allows for relatively high porosity and larger surface area. The formation in a gel environment allows for better synthesis of nanostructures. Zirconium is chosen for the transition metal as it is a cheaper alternative to titanium which possesses similar qualities at a higher price range [8].

In order to achieve the goal product, the work was divided into stages:

- Using sol gel method to synthesize the precursor zirconium carbide.
- Find out the correct amount of alkoxide and carbon source (hydroquinone) required for the formation of stoichiometric zirconium carbide.
- Continue with further steps of pyrolysis, carbothermal reduction and chlorination to get carbon as our final material.
- Characterize the obtained ZrC material, using X-ray diffraction method, sorption measurements and scanning electron microscopy.
- Characterize the final carbon material obtained via chlorination, using X-ray diffraction method, Raman spectroscopy, sorption measurements and scanning electron microscopy.

The aim is to synthesize zirconium carbide derived carbon (ZrC-CDC) using sol gel method for the synthesis of the precursor carbide to analyze and characterize the resulting carbon material for the use as an electrode material for a supercapacitor.

The author has independently performed all precursor carbide and carbon syntheses and interpreted XRD diffractograms, Raman spectra, SEM images and data from the sorption measurements obtained during sample characterization. The content of the work has been written and formatted by the author independently. In collaboration with the supervisor, the appropriate synthesis parameters and specific advice from the tutor for synthesizing samples and drawing conclusions have been established in advance. The safety of the work was ensured by meeting all the requirements for working in the laboratory, in additional consultation with the relevant specialists.

2. Literature overview

The literature overview is based on professional scientific literature and articles that have been found on databases such as ScienceDirect, Sigma Aldrich, and Academia with the use of Google as a search engine.

2.1 Carbides

Carbides can be defined as a composition of carbon and less electronegative elements, mainly prepared with metals at relatively high temperatures of 1000-2800 °C for industrial uses [9]. Their qualities usually depend on the other contributor as within the forming process carbon has a tendency to adapt and copy the other compound's qualities. This makes our choice of the other compound quite significant, as we will be focusing on getting the carbon out of this carbide later on in our experiments.

There are several methods to prepare carbides and the majority of the carbides can be prepared with the following methods. The first method would be to directly combine our elements at 2000°C or above. The second method would be by using the oxide of the metal and then combining them at a high temperature. Other interesting methods worth mentioning include the reaction of a metal salt with a hydrocarbon and the dissolving of metal in liquid ammonia where the hydrocarbon would be bubbled through the solution. Still, all these methods will include high temperatures as we are making structural changes and formations within the compound [5].

Different methods yield different results when it comes to the properties of the resulting carbide depending on how efficiently the reaction is carried out. This makes the classification of carbides quite challenging based on structure. The classification of carbides can be determined through the contributing element. The more electropositive metals would form ionic (saltlike) carbides, the transition metals would form interstitial carbides and nonmetals that would qualify for the electronegativity to form a carbide would form covalent (molecular) carbides [10]. The class of interest for the purposes of our paper are interstitial carbides.

2.1.1 Interstitial carbides and transition metals

Interstitial carbides are derived from transition metals within the periodic table. Transition metals are elements that possess partially filled d orbitals [11]. We see them on the d block of the periodic table. From the periodic table, we can make a comment on trends based on the gradual change we observe across the table from left to the right. With their relative position on the table and by comparing to the rest of the elements we can come to conclusions about the properties of transition metals [12].

The properties of transition metals can be listed as possessing a large charge/radius ratio, high density, elevated melting, and boiling points as well as forming stable complexes and showing variable oxidation states. The high density can be explained by the increase in atomic mass and decrease in metallic radius. The melting point and molar enthalpies being as high as they are due to the strong metallic bonding that would occur due to the delocalization of electrons managed by the availability of s and d electrons [13].

Majority of these properties can also be seen in interstitial carbides. The transition metal in the case of interstitial carbides acts as a host for small carbon atoms. Due to the high density of transitional metals, they are extremely stiff yet brittle and keep most of the metal's properties such as high melting temperatures, heat and electricity conductivity and even in some cases, the metal can manifest itself as a sheen in the final compound. Unlike other carbide classes, interstitial carbides do not react with water and are chemically inert as well [14].

All these properties give interstitial carbides great importance in industrial applications, but we intend to go further and try to get the final compound as carbon that possesses these qualities on its own, therefore, its carbide derived carbon (CDC), using the carbide as a precursor [15]. Considering the applications we wish to implement over CDC, we favored the sol-gel method for the carbide synthesis.

2.2 Sol gel method

The sol gel process is a wet chemical method where the molecular precursor is dissolved and then converted to a gel. This gel then goes through thermal treatments to be converted into solid materials. This method is mainly used for the synthesis of nanostructures specifically metal oxide nanoparticles but can be used in the preparation of nitrides, carbides, fluorides etc [16].

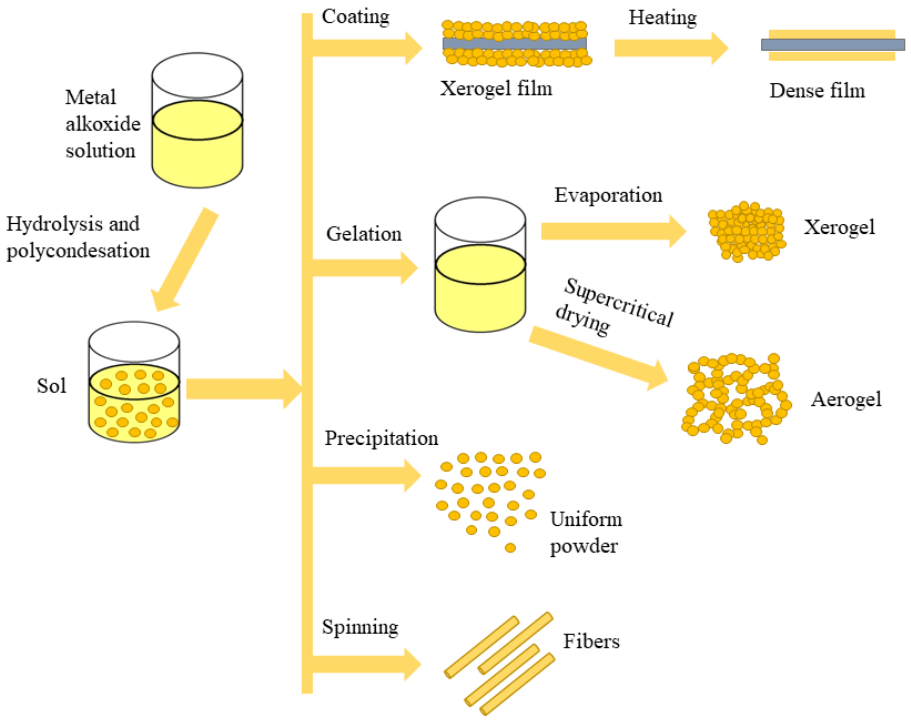

Figure 1. Sol gel synthesis [17].

Sol-gel method relies on the hydrolysis and condensation of the precursor sol which then through a series of reactions and heating turns into a gel. The two main reactions that evidently control the chemical and physical properties of the obtained product are the hydrolysis of the precursor in acidic or basic mediums and then polycondensation of the hydrolyzed products [18]. These two main reactions result in clusters forming and binding to each other, forming a gel that increases in viscosity as time passes on. We can observe within the steps of the process the change from solution to gel [19].

The process carries out as [16] [19]:

- Preparation of the solution of precursors.
- Hydrolysis and partial condensation of alkoxides to form a "sol".
- Formation of the gel via polycondensation of hydrolyzed precursors.
- Drying. The gel forms a dense "xerogel" via collapse of the porous network caused by the evaporation of the solvent (or an aerogel for example through supercritical drying).

The sol gel method is particularly of interest lately due to the high surface area, lower synthesis temperatures and low production costs [20].

2.2.1 Sol-gel method for metal alkoxides

The sol-gel method of metal alkoxides relies mainly on the hydrolysis of the metal alkoxide. The first product that forms is a xerogel, an amorphous hydrated compound with alkoxide group. The drying and pulverizing of this compound gives us an easily manageable powder. Therefore, it can be said that the majority of the characteristics of the final product depend on the hydrolysis. The metal alkoxide used also matters a lot as it sets the base qualities. The molecular structure and complexity determine the characteristics of the future product. Although at first the sol-gel method was used mostly for the hydrolysis of $Si(OR)_4$, metal alkoxides and their modified versions have become the most frequently used ones nowadays [21].

The most commonly used precursors for the sol-gel method are usually alkoxides, $M_x(OR)_y$. They are particularly good for the chemical control of oxide synthesis since due to the high electronegativity of oxygen with respect to the metal M-O-C bonds are polarized and so the reaction rates are high. The alkoxide is mainly responsible for the control of the stoichiometry and homogeneity [22]. The reactivity that the final product will have mainly depends on the alkyl group R and can be chosen from an almost infinite number of groups [23].

The reaction process of sol-gel method for metal alkoxides in detail follows through hydrolysis with the generation of a metal hydroxy group via reaction 1:

$$M\text{-}(OR)_n + nH\text{-}OH \rightarrow M\text{-}(OH)_n + nR\text{-}OH. \quad (1)$$

This will be followed by polycondensation as previously mentioned, however polycondensation itself has 3 competitive mechanisms, depending on the chemical conditions of

the reaction, alcoxolation, oxolation, and olation [13]. Alcoxolation is when a hydrolysed precursor reacts with the alkoxy precursor as seen in reaction 2:

$$M\text{-}OH + M\text{-}OR \rightarrow M\text{-}O\text{-}M + R\text{-}OH, \quad (2)$$

Oxolation is when the hydrolyzed precursor reacts with another hydrolyzed precursor, shown in Reaction 3:

$$M\text{-}OH + M\text{-}OH \rightarrow M\text{-}O\text{-}M + H\text{-}OH, \quad (3)$$

Olation is when the elimination of the solvent molecule forms bridging hydroxo groups as in reaction 4:

$$M\text{-}OH + M \rightarrow M\text{-}O\text{-}M + R\text{-}OH. \quad (4)$$

2.3 Carbide derived carbon

Carbide derived carbons (CDCs) can be defined as a group of carbon materials that are achieved by eliminating the metal component to leave pure carbon behind. This elimination process can be through physical processes such as thermal decomposition or through chemical processes such as halogenation [24].

The structural properties of CDC can be from porous to dense, amorphous to crystalline and from sp^2- to sp^3-bonded [25]. The structural and porous properties of the resulting product would depend on synthesis conditions and the carbide precursor. By optimizing and varying the synthesis conditions and using different carbides as precursor the micro- and mesoporosity, average pore size and pore size distributions can be controlled [26], [27]. Previously mentioned parameters and the high electric conductivity and electrochemical stability of CDCs makes them extremely attractive for uses in different energy storage devices as electrode materials.

Within the energy storage, one area of interest for CDC applications is as active electrode materials in electric double layer capacitors due to their properties such as large micropore volume, high surface area and more. The high electric conductivity that CDC provides would minimize the resistance losses in supercapacitors and maximize the density and charge storage capacity of the electrodes [28]. The control over pore size allows to tune the parameters of the electrode to a particular electrolyte.

Literature has presented examples of high-power supercapacitor electrodes based on TiC-CDC nano felts [29]. Zirconium carbide derived carbon (ZrC-CDC) can also be used as electrode

material and shows relatively similar characteristics [30]. In production using sol gel method, the cost of titanium carbide (TiC) is higher when compared to ZrC. As the properties of CDC can be modified by altering the synthesis conditions and the carbide precursor, the attention shifts from TiC-CDC to the synthesis of ZrC-CDC in a controlled manner to produce the electrode material with desired characteristics.

The alterations that are needed for the carbon synthesis of a carbide material can happen in two stages, within the extraction of the metal and within the synthesis of the carbide precursor. One of the methods to eliminate the metal is through electrochemical etching. Electrochemical etching in contrast to the more commonly used chlorination method, where the gas forms a compound with the metal to get rid of it, happens at ambient temperature and does not require gas [31], [32]. Throughout this process the metal atoms are selectively extracted from the ternary layered carbides by electrochemically inducing them.

Chlorination is a kind of halogenation reaction specifically occurring with chlorine. Halogenation can be described as a chemical reaction where the halogen of choice is introduced to the environment with the precursor and with nothing else [33]. The purpose is to form a reaction where the halogen of choice will react with the material and the final result is carbon material. Within the halogens, fluorine and chlorine are the most aggressive ones as they are the more electrophilic ones. Still, chlorine is slightly selective but reacts fine with most metals and heavier nonmetals.

2.3.1 Uses of carbide derived carbons

The fine tunability of parameters such as pore sizes makes CDC extremely attractive for uses in many fields ranging from energy and material applications to biomedical applications further into the industrial fields [34].

The proposed applications of CDC are quite vast and promising. Research has shown that CDC films obtained by vacuum annealing (ESK) or chlorine treatment of SiC ceramics yield a low friction coefficient and so offer use in tribological coatings [35]. Besides material applications, CDCs with a mesoporous structure can remove large molecules from biofluids as they possess great biocompatibility. They can remove certain cytokines that are in the blood plasma that are

mostly responsible for the inflammatory response, making their removal extremely critical and playing a part in protein adsorption [36].

A solid application of carbide derived carbons is as an electrode material in electrical double layer capacitors. Also known as supercapacitors, electric double-layer capacitors are used in energy storage. The superior electrical conductivity, high surface area, large micro- and mesopore volume and pore size tunability to the appropriate electrolyte makes CDC desirable for such applications. The tunable porosity is the main feature of CDC that we focus on. Particularly with pore size, when the pores approach the ions in the electrolyte there is an increase in capacitance [37]. The active electrode material minimizes resistance losses, enhances charge screening and confinement, maximizing the packing density and subsequent charge storage capacity of microporous CDC electrodes [38].

3. Experimental

3.1 Synthesis of carbide derived carbons

The work at hand uses sol gel method to synthesize zirconium carbide. The zirconium carbide then goes through thermal treatments and further chlorination to acquire micro-mesoporous zirconium carbide derived carbons.

3.1.1 Sol gel synthesis of zirconium carbide precursor

For the synthesis of zirconium carbide precursor zirconium (IV) butoxide solution, ($Zr(OC_4H_9)_4$ 80 wt% in 1-butanol, Alfa-Aesar), was used as metal source; benzene-1,4-diol, ($C_6H_4(OH)_2$, 99% purity, Sigma-Aldrich), as a carbon source; and as chelating ligand acetylacetone ($C_5H_8O_2$, $\geq$ 99%, Sigma-Aldrich) was used.

0.0484 mol $Zr(OC_4H_9)_4$ was dissolved in 0.2646 mol 1-butanol under argon in a three-neck flask. The solution was heated up to 50°C when the solution environment butanol and the metal source is added and then raised to 80°C with the addition of acetylacetone to control the alkoxide hydrolysis. Later the carbon source is added and so the temperature is once again raised, this time to 120°C for 2 hours for the reaction to take place. The temperature is then raised to 150°C for the distillation of butanol to take place and for the xerogel to be fully dry. Once the xerogel is dry it is powdered with a mortar and pestle for the thermal treatments.

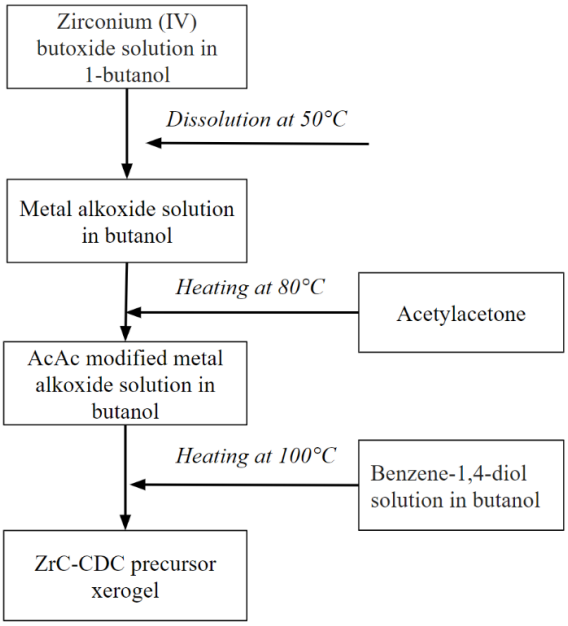

Figure 2. The scheme for the synthesis of zirconium carbide precursor xerogel.

3.1.2 Pyrolysis, carbothermal reduction and chlorination

The powdered xerogels were heat treated (pyrolyzed) at 800 °C under argon atmosphere for 1 h. The heating rate was adjusted to 200 °C h^{-1}.

ZrC precursor → 800 °C → ZrO_2 + C (5)

The pyrolyzed samples go through carbothermal reduction at 1300 °C in vacuum at 10^{-2} mbar in a tube furnace and the carbothermal reduction time at the maximum temperature was 60 min. The heating rate was adjusted to 200 °C h^{-1}.

ZrO_2+3C → 1350°C → ZrC+2C↑ (6)

The synthesized zirconium carbides were placed onto a quartz stationary bed reactor and reacted with a steady flow of Cl_2 (AGA, 99.99%). Three different chlorination temperatures were used, T_1 = 700 °C, T_2 = 800 °C and T_3 = 900 °C.

ZrC + 2Cl_2 → T_1,T_2,T_3→ C + $ZrCl_4$ (7)

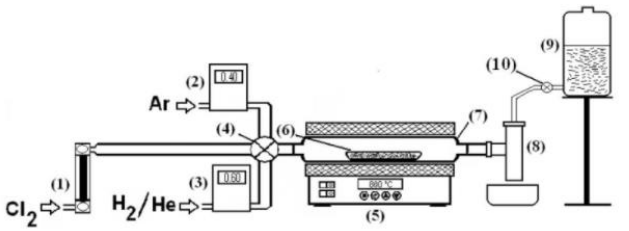

1) Chlorine flow meter, 2) Argon flow meter, 3) Hydrogen flow meter, 4) tap, 5) tube furnace, 6) quartz boat with the sample, 7) quartz tube, 8) neutralization vessel, 9) neutralization solution vessel, 10) neutralization vessel's tap.

Figure 3. Chlorination setup.

The flow rate of Cl_2 was fixed at 50 ml min^{-1}. During heating up and cooling down steps, the reactor was flushed with argon (300 ml min^{-1}). The resulting CDC was thereafter treated with H_2 at 900 °C for 1h to dechlorinate thoroughly the CDC powders as well as to remove the residual chlorides, chlorine and oxygen-containing functional groups from the surface of the porous carbon under study.

4. Results

4.1 Precursor analysis

The precursor material was analyzed and adjusted to fit the necessary conditions to carry on with the experiments.

4.1.1 Molar ratio analysis

For the experiments and the synthesis of the ZrC precursor material, the carbon source and the metal oxide source needs to have a molar ratio of $C/ZrO_2 = 3$. The added amount of the carbon and metal oxide sources were varied to determine the ratio that is needed. After pyrolysis, the samples varying in carbon and metal oxide amounts were burnt in air to then calculate the molar ratio. In the end, 0.5 mols were determined for the right ratio.

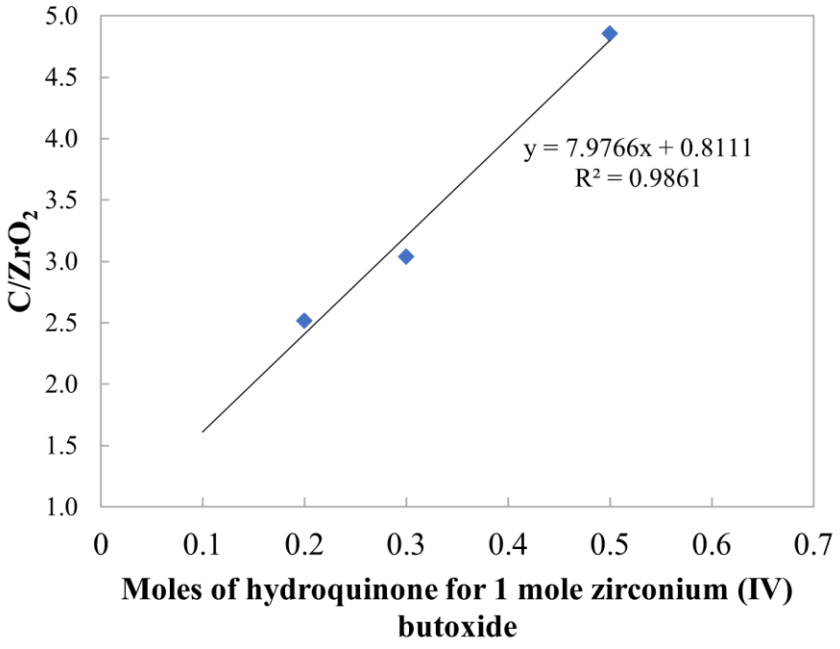

Figure 4. Molar ratio graph.

4.1.2 Infrared spectroscopy analysis of the precursor materials

To ensure that the synthesis part of our experiments went accordingly, 3 samples were randomly selected to be analyzed.

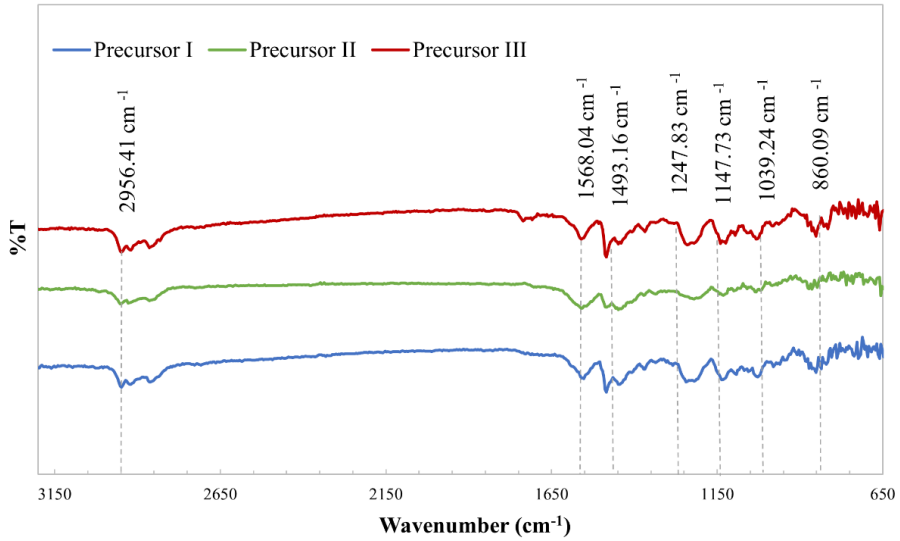

Figure 5. IR spectra of three precursor samples.

In Figure 5 the IR spectra of precursor xerogel materials show the absorption bands starting from 2956.42 cm^{-1}. From 2700 cm^{-1} to 1600 cm^{-1} we don't see any absorption bands. From 1590 cm^{-1} to 1530 cm^{-1} we can see that the C=O and C=C bonds in acetylacetone have bonded it to the Zr [39]. With that, the absorption bands at 1493.16 cm^{-1} and 1247.83 cm^{-1} show the bonding of benzene-1,4-diol to the Zr [40]. Bands from 1154 cm^{-1} to 1020 cm^{-1} are assigned to Zr-O-C interactions [40]. The signals received on the low energy side of the spectra, below 950 cm^{-1} are suspected to be due to of different Zr–O–Zr bonds [41].

4.2. Characterization of zirconium carbide materials

4.2.1. X-ray diffraction method

Selected carbides were analyzed using X-ray diffraction (XRD) to determine that they are indeed carbides. The XRD analysis was performed using CuKα radiation (45 kV, 35 mA, λ = 0.154056 nm) with a step size 0.013 2θ and with the total counting time of 178 seconds per step on Bruker D8 Advance diffractometer.

Comparing our samples to the commercial ZrC show us that our carbide bonds were perfectly placed and aligned to where they should be. The varying levels of oxide bonds in ZrC-I, ZrC-II and ZrC-III are mostly due to residual zirconium oxide in the carbide. Through thermal treatments (carbothermal reduction) we expected these oxide peaks to disappear.

The height of the peaks in comparison to the commercial carbide are promising, since the higher the peak is the more crystalline the material is [42]. The peaks of ZrC-I, ZrC-II and ZrC-III show to be broader and lower, suggesting that it is much more amorphous and less crystalline [43] in comparison to the commercial one, making it a better fit for applications.

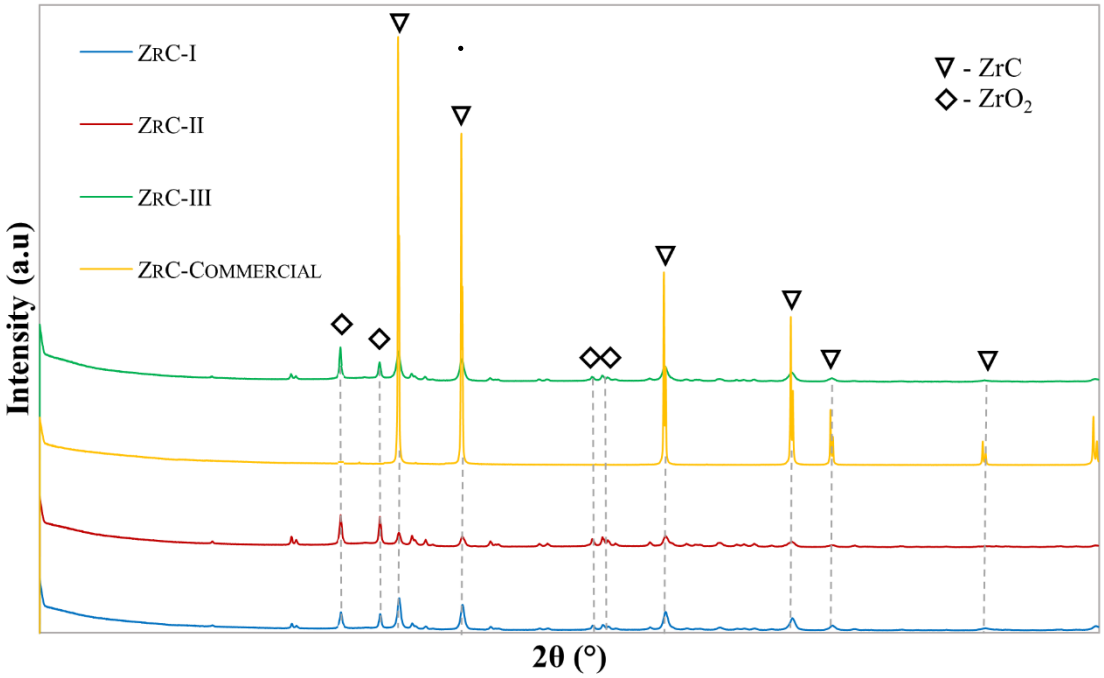

Figure 6. XRD peaks of obtained ZrC material.

4.2.2 Sorption measurements data

The samples that were synthesized were then further analyzed with liquid nitrogen sorption measurements. The sorption measurements were carried out in a low temperature nitrogen enviroment using 3FLEX (micromeritics) and specific surface areas have been calculated according to the Density Functional Theory while still using the BET model for better comparison [44], [45] to the already existent data. Pore size distributions were calculated through the application of non-local density functional theory on N_2 adsorption isotherms.

Sample	S_{BET} / m^2 g^{-1}	S_{DFT} / m^2 g^{-1}	V_{tot} / cm^3 g^{-1}	V_{DFT} / cm^3 g^{-1}
ZrC-I	63	63	0.11	0.10
ZrC-II	69	63	0.11	0.10
ZrC-III	65	62	0.11	0.10

Table 1. Liquid nitrogen sorption measurements data for zirconium carbides.

The specific surface area for both samples were calculated according to BET and DFT, although the S_{DFT} stayed the same for both samples, S_{BET} did slightly differ by 6 m^2g^{-1}, displaying a higher surface area for ZrC-II. The specific volume was also calculated, giving the same results, and once again showcasing the sustainability of sol-gel method for such synthesis. The commercial ZrC showed such low measurements that the porosity measurements were not taken into account and only the total volume could be measured at 0.002552 cm^3/g, showing that in comparison sol-gel synthesized had much more suitable porosity qualities.

In Figure 7, we can see that the materials show microporous and mesoporous composition of the carbides. The pore size distribution showed that the three samples had very similar characteristics in mesopores with an even distribution of mesopores above 2 nm, ZrC-I having a larger amount in comparison from 1 to 5 nm. The overall pattern of distribution was almost the same with ZrC-I and ZrC-III, ZrC-I had a higher the distribution of pores from 0.4 nm to 0.6 nm yet further, ZrC-III seemed to have a higher distribution of the rest. The other two samples showed difference in the distribution of micropores, ZrC-I had a lot more micropores than ZrC-II, reaching the maximum at 0.55 and having gotten less as the pores get larger. Still, ZrC-II showed a much larger concentration of micropores from 0.63 to 1 nm.

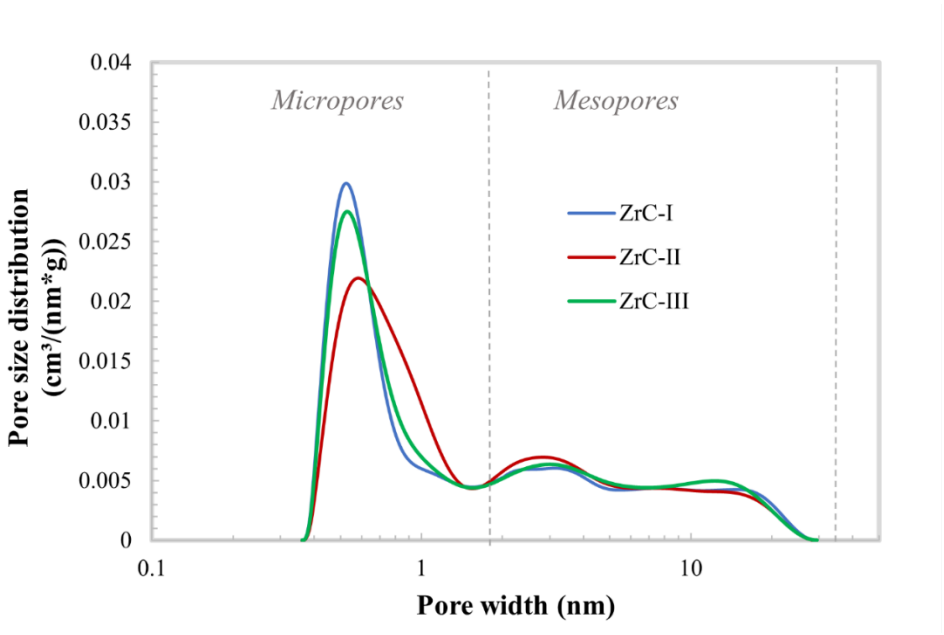

Figure 7. Pore size distribution vs. pore width plots for carbides.

4.2.3 Scanning electron microscopy

The SEM analysis was carried out using Zeiss EVO MA 15. The samples were coated in a thick layer of platinum about 5-10 nm using Leica EM SCD500 high vacuum sputter coater for a higher vacuum. The necessary accelerating voltage was 20kV and the secondary electron detector was used to capture the images.

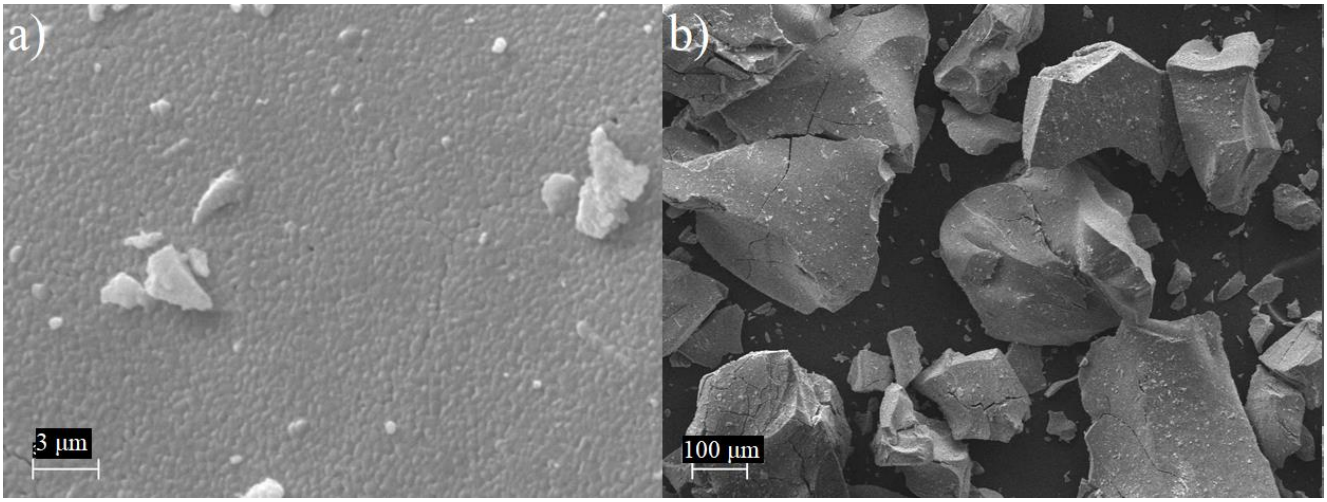

Figure 8. SEM images of obtained ZrC material a) ZrC at 10kx, b) ZrC at 250kx.

The obtained ZrC material seemed to have relatively smooth particles with sharp edges, being around 200 to 300 μm on average. Further up close we can see a very porous surface subtle cracks and ridges on the surface in a relatively uniform manner, staying in the microporous side with most of the smaller pores being smaller than 1 μm.

4.3. Characterization of zirconium carbide derived carbon materials

4.3.1 X-ray diffraction method

The obtained carbons were analyzed using X-ray diffraction (XRD). The XRD analysis was performed using CuKα radiation (45 kV, 35 mA, λ = 0.154056 nm) with a step size 0.013º2θ and with the total counting time of 178 seconds per step on Bruker D8 Advance diffractometer.

Referring to Figure 6 we see the oxide peaks from the carbide in the carbon material that should have gone through the thermal treatments. Here, we can clearly see the importance of correct temperature for thermal treatments as ZrC-CDC 800 °C shows to be a great example of amorphous carbon without peaks, however, we can see with ZrC-CDC 700 °C and ZrC-CDC 900 °C that this is not the case.

Both of the samples have relatively the same oxide bonds at given places, as a residue most likely. The interesting peak at ZrC-CDC 700 °C is the oxide bond indicating Tazheranite, an isometric zirconium crystal. The bonding we see in ZrC-CDC 900 °C and in the other peaks of ZrC-CDC 700 °C indicates Baddeleyite form of the zirconium oxide, a monoclinic crystal. The changing factor being the heat we could have said that as the chlorination temperature increases the oxide bonds go away as so but the broad and smooth spectra of ZrC-CDC 800 °C would disprove this.

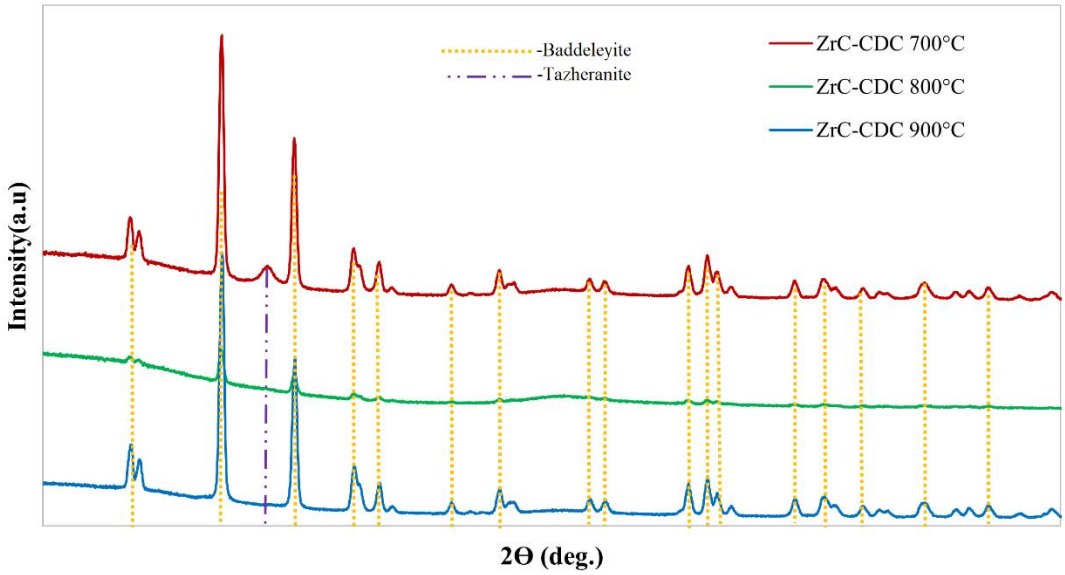

Figure 9. XRD patterns for the final obtained ZrC-CDC at 700 °C, 800 °C, 900 °C.

4.3.2 Raman spectroscopy

The Raman spectra for the final carbon samples at different chlorination temperatures was obtained with excitation using Renishaw inVia Raman spectrometer. The setup was equipped with a 514 nm continuous mode argon ion laser, the laser power at sample was set at 1.3mW and the spectral resolution was approximately 1.5 cm^{-1}.

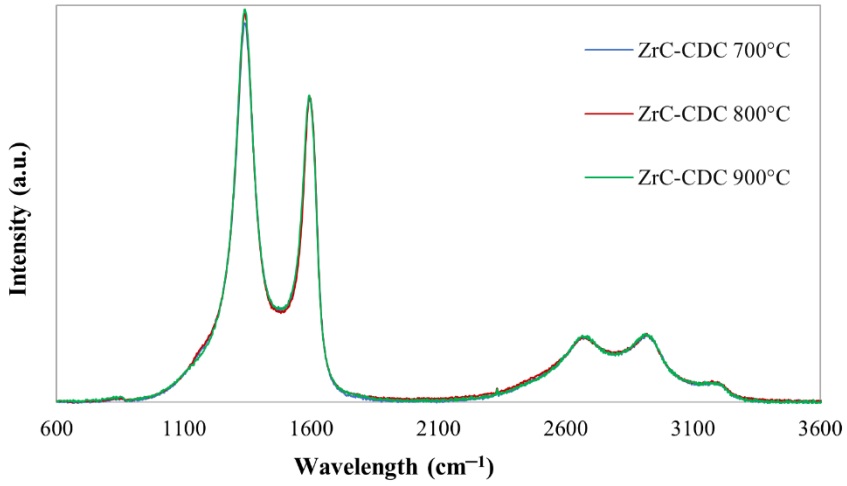

Figure 10. Raman spectra for the final obtained ZrC-CDC at 700 °C, 800 °C, 900 °C.

The spectra were normalized according to the G peak, allowing us to see that structurally, the samples are extremely alike. The spectrum shows two strong peaks at approximately 1360 cm^{-1} and 1600 cm^{-1} apparent as the D- and G-peaks and the 2D peaks are visible from 2350 cm^{-1} to 3250 cm^{-1}. From the slight differences in between peaks, we can say that ZrC-CDC 700 °C had the lowest intensity with ZrC-CDC 800°C being higher and ZrC-CDC 900 °C being the highest Still, in a behavioral sense, we see that ZrC-CDC 700 °C, ZrC-CDC 800 °C and ZrC-CDC 900 °C seem to be similar.

4.3.3 Sorption measurements data

The final obtained carbon at 3 different temperatures also went through sorption measurements in a low temperature nitrogen enviroment using 3FLEX (micromeritics). The specific surface areas have been calculated according to the Density Functional Theory while still using the BET model [44], [45] for better comparison to the already existent data. Pore size distributions were calculated through the application of non-local density functional theory on N_2 adsorption isotherms.

Sample	S_{BET} **m²/g**	S_{DFT} **m²/g**	V_{tot} **cm³/g**	V_{DFT} **cm³/g**
ZrC-CDC 700 °C	1290	1140	2.04	1.90
ZrC-CDC 800 °C	1570	1290	2.48	2.29
ZrC-CDC 900 °C	450	370	0.75	0.70

Table 2. Sorption measurements for CDCs at different temperatures.

S_{BET}, S_{DFT}, V_{DFT} and V_{tot} was calculated for all samples. We can see from the table that ZrC-CDC-800°C showed the highest results and ZrC-CDC 900 °C the lowest for all measurements. The specific surface area for all samples were calculated according to BET and DFT, and for both measurements ZrC-CDC 700 °C displayed specific surface area above 1100 m²/g, however as the measurements for ZrC-CDC 900 °C was lower than 500 m²/g, we can say that 900 °C was the least optimal temperature for chlorination. The measurements for S_{BET} and S_{DFT} did differ with S_{DFT} measurements being on average 16% less. The measurements also varied between V_{tot} and V_{DFT}, with DFT measurements again being lower for all samples. Still as it is more sensitive, taking DFT measurements into account, 800 °C was the best selected chlorination temperature as the data suggests great porous qualities.

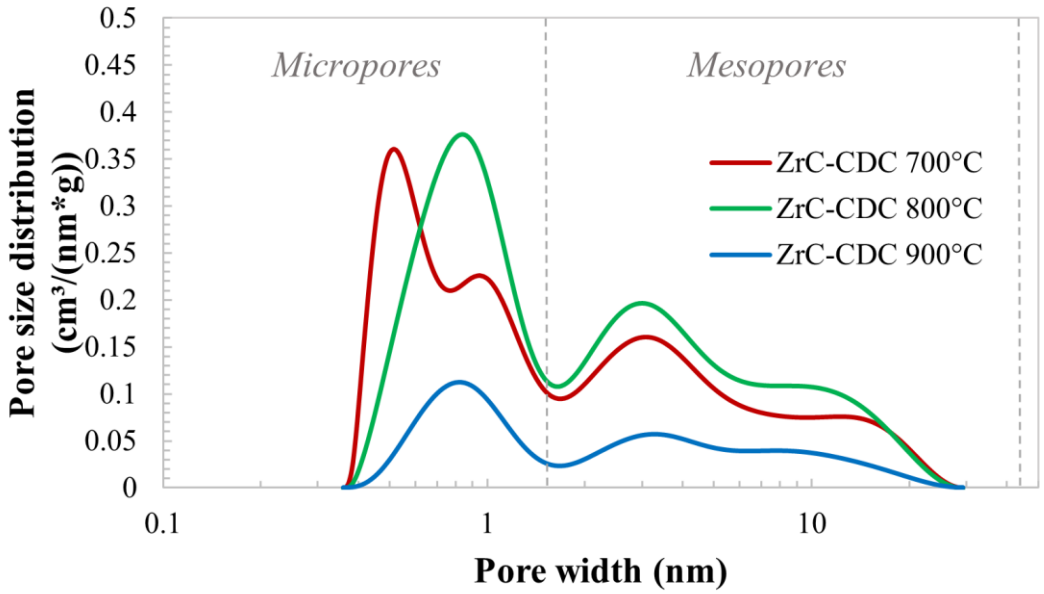

Figure 11. Pore size distribution to pore width plots for the final obtained ZrC-CDC at 700 °C, 800 °C, 900 °C.

The samples differ in distribution in both micropores and mesopores. Out of all three samples ZrC-CDC 800 °C showed the most even distribution of pores with the lowest distribution being in ZrC-CDC 900 °C. ZrC-CDC 700 °C had the most pores until 0.6 nm, from then on until 1 within micropores ZrC-CDC 800 °C had the most and ZrC-CDC 700 °C had a varying distribution. From 1 nm and above the distribution patterns of the samples are quite similar, just varying in amounts with ZrC-CDC 800 °C having the most and ZrC-CDC 900 °C having the least.

4.3.4 Scanning electron microscopy

The SEM analysis was carried out using Zeiss EVO MA 15. The samples were coated in a thick layer of platinum about 5-10 nm using Leica EM SCD500 high vacuum sputter coater for a higher vacuum. The necessary accelerating voltage was 20kV and the secondary electron detector was used to capture the images.

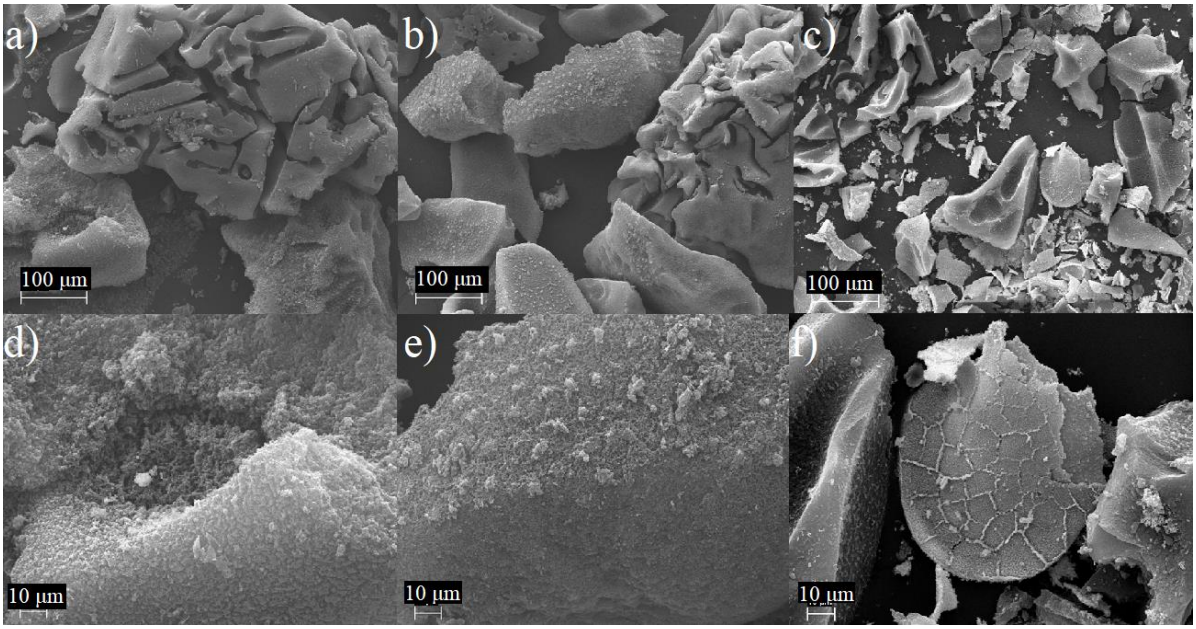

Figure 12. SEM images of the final carbon a) ZrC-CDC 700 °C at 500x, b) ZrC-CDC 800 °C at 500x, c) ZrC-CDC 900 °C at 500x, d) ZrC-CDC 700 °C at 2kx, e) ZrC-CDC 800 °C at 2kx, f) ZrC-CDC 900 °C at 2kx.

From the given images we can comment that the ZrC-CDC 700 °C showed to have many crevasses on the surface, rigids inside and out of big relatively smooth edges between the ridges. From afar, theses ridges create almost a fuzzy texture on the surface, covering it almost completely, in a uniform manner. For ZrC-CDC 800 °C we see a similar behavior more sporadically and ordered. The crevasses are still apparent but the particle itself that the crevasses are on is almost half the size in comparison to ZrC-CDC 700 °C and from afar the porous layout and texture on the main surface seems much more organized. In contrast to both, ZrC-CDC 900 °C appeared to be just small broken up pieces with rough edges and grooves in the surface, resembling what might have been a similar layout to ZrC-CDC but as if it had been shattered to pieces and from afar it did not resemble either of the other samples.

4.3.5 Transmission electron microscopy

The transmission electron microscopy (TEM) images in Figure 13 show the uniformity and the spread of the microstructure much clearly as it is more sensitive. From Figure 13, we can see

that ZrC-CDC at 700 °C is mainly composed of an amorphous part and from some more crystalline particles. The sample exhibited broad size distribution of particles. The amorphous part seems to be made of very thin crumpled layers of materials, maybe just a few atoms thick. The sample ZrC-CDC 800 °C is very similar to ZrC-CDC 700 °C. The main difference comes from the observation of fewer crystalline particles. Also, the ZrC-CDC 900 °C is similar to previous ones, with a majority of amorphous particles and only a few crystalline particles.

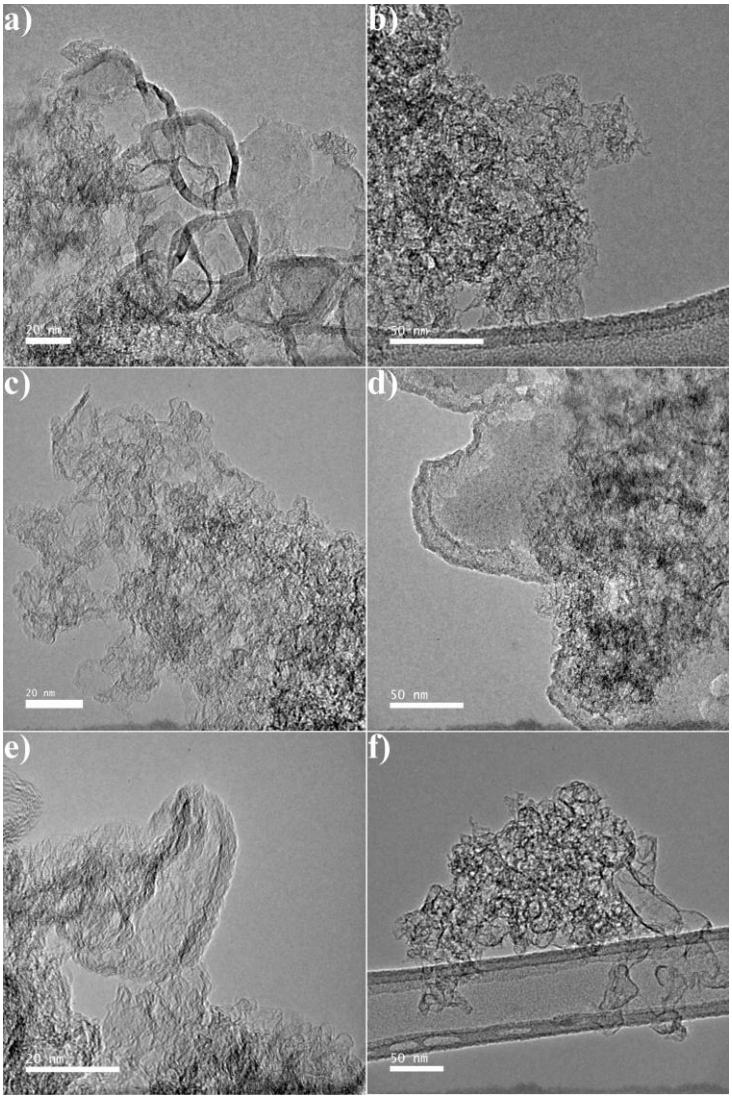

Figure 13. Transmission electron microscopy pictures of a) ZrC-CDC at 700 °C at 20 nm, b) ZrC-CDC at 700 °C at 50 nm; c) ZrC-CDC at 800 °C at 20 nm, d) ZrC-CDC at 800 °C at 50 nm; e) ZrC-CDC at 900 °C at 20 nm, f) ZrC-CDC at 900 °C at 50 nm.

5. Conclusions

The aim of the thesis was to use sol-gel method for the synthesis of zirconium carbide (ZrC) precursor material that would go through thermal treatments such as pyrolysis, carbothermal reduction and chlorination for the final zirconium carbide derived carbon (ZrC-CDC) to be obtained.

The necessary molar ratio for sol-gel ZrC precursor material was determined to be 0.5 mols. The precursors that went through pyrolysis were analyzed and the pyrolysis process successfully resulted in carbides. The carbide samples were further analyzed with XRD. In comparison to the commercial one the sol-gel synthesized ones showed more amorphous properties. The pore size distribution plots showed the samples to have similar characteristics, with only slight difference between the microporosity of samples. This was reasoned by the fact that ZrC-I and ZrC-II happened to have ~ 0.08 mols excess zirconium butoxide. Referencing SEM images of commercial TiC in studies [46], compared to the irregular distribution of particles in commercial TiC, sol-gel synthesized ZrC appeared to be less textured with smoother edges.

Following pyrolysis and carbothermal reduction the samples went through chlorination at 3 different temperatures 700 °C, 800 °C, 900 °C. The XRD pattern for the samples showed 800 °C to be the ideal temperature as the diffraction peaks were broader showing great amorphous properties compared to samples at 700 °C and 900 °C degrees as they differed from 800° C in a similar way, still possessing oxide in its carbon structure. 800° C being the best out of selected chlorination temperatures was also supported by SEM and TEM results.

The successful sol-gel synthesized ZrC-CDC showed great qualities compared to the commercial brand at lower production costs. The sol-gel method allowed for lower synthesis temperatures, a larger surface area and contributed heavily to the porous and structural qualities of the final carbon, making it an eligible method for the synthesis of ZrC-CDC for applications in supercapacitors as electrode material.

6. Synthesis of zirconium carbide derived carbon using sol-gel method, carbothermal reduction and chlorination

Selin Su Yegit

Summary

The aim of the thesis was to synthesize zirconium carbide (ZrC) as a precursor to zirconium carbide derived carbon. The decided method to do so was sol gel method due to its low cost and low temperature applications. The precursor zirconium carbide went through the necessary thermal treatments determined as pyrolysis, carbothermal reduction and chlorination, to obtain the final carbon. Different conditions were studied for the thermal treatments to study the different outcomes. The precursor ZrC and the final carbon were characterized by X-ray diffraction, Raman spectroscopy, sorption measurements, scanning electron microscopy (SEM) and transmission electron microscopy (TEM).

The following conclusions were made:

- It was determined for the rest of the treatments to carry on the right molar ratio for zirconium butoxide and benzene-1,4-diole was 1 to 0.55 moles.
- The suitable method to carry on with the synthesis was determined to be sol-gel technique.
- IR results confirmed that the sol-gel method is repeatable for the synthesis of ZrC precursor material.
- X-ray diffraction analysis showed the necessary carbide peaks in ZrC and provided insight into choosing the right chlorination temperature.
- Sorption measurements showed the material to be micro- and mesoporous carbon.

7. Acknowledgements

I would like to first thank my supervisor Maarja Paalo for her mentorship and guidance as well as Meelis Harmas for introducing me to the topic. I would additionally like to express my gratitude towards all the people that helped with the analysis process: Jaan Aruväli for X-ray diffraction, Tavo Romann for Raman spectroscopy and infrared results, Miriam Koppel for sorption measurements and Marian Külaviir for scanning electron microscopy.

8. References

[1] S. Huang, X. Zhu, S. Sarkar, and Y. Zhao, "Challenges and opportunities for supercapacitors," *APL Materials*, vol. 7, no. 10, Oct. 2019, doi: 10.1063/1.5116146.

[2] W. Gu, X. Wang, and G. Yushin, "Nanostructured Activated Carbons for Supercapacitors," 2015.

[3] E. Redondo, L. W. L. Fevre, R. Fields, R. Todd, A. J. Forsyth, and R. A. W. Dryfe, "Enhancing supercapacitor energy density by mass-balancing of graphene composite electrodes," *Electrochimica Acta*, vol. 360, p. 136957, Nov. 2020, doi: 10.1016/J.ELECTACTA.2020.136957.

[4] S. Hérou *et al.*, "High-Density Lignin-Derived Carbon Nanofiber Supercapacitors with Enhanced Volumetric Energy Density," *Advanced Science*, vol. 8, no. 17, Sep. 2021, doi: 10.1002/ADVS.202100016.

[5] Y. Xiao, J. Y. Hwang, and Y. K. Sun, "Transition metal carbide-based materials: Synthesis and applications in electrochemical energy storage," *Journal of Materials Chemistry A*, vol. 4, no. 27, pp. 10379–10393, 2016, doi: 10.1039/C6TA03832H.

[6] S. Rajagopal, R. Pulapparambil Vallikkattil, M. Mohamed Ibrahim, and D. G. Velev, "Electrode Materials for Supercapacitors in Hybrid Electric Vehicles: Challenges and Current Progress," *Condensed Matter 2022, Vol. 7, Page 6*, vol. 7, no. 1, p. 6, Jan. 2022, doi: 10.3390/CONDMAT7010006.

[7] U. Jansson and E. Lewin, "Sputter deposition of transition-metal carbide films — A critical review from a chemical perspective," *Thin Solid Films*, vol. 536, pp. 1–24, Jun. 2013, doi: 10.1016/J.TSF.2013.02.019.

[8] G. R. Lee and J. A. Crayston, "Sol-gel processing of transition-metal alkoxides for electronics," *Advanced Materials*, vol. 5, no. 6, pp. 434–442, 1993, doi: 10.1002/ADMA.19930050604.

[9] "carbide | chemical compound | Britannica." https://www.britannica.com/science/carbide (accessed Apr. 03, 2022).

[10] "Carbides: Properties, Production, and Applications - T. Y. Kosolapova - Google Books." https://books.google.ee/books?hl=en&lr=&id=6_HTBwAAQBAJ&oi=fnd&pg=PA2&dq=classification+of+carbides&ots=4-AAEsFYNg&sig=nvWGf1e7zc-HJYQuNW2LWERzmSQ&redir_esc=y#v=onepage&q=classification%20of%20carbides&f=false (accessed Apr. 03, 2022).

[11] J. G. Chen, "NEXAFS investigations of transition metal oxides, nitrides, carbides, sulfides and other interstitial compounds," *Surface Science Reports*, vol. 30, no. 1–3, pp. 1–152, Jan. 1997, doi: 10.1016/S0167-5729(97)00011-3.

[12] W. Leal and G. Restrepo, "Formal structure of periodic system of elements," *Proceedings. Mathematical, Physical, and Engineering Sciences*, vol. 475, no. 2224, 2019, doi: 10.1098/RSPA.2018.0581.

[13] P. Parisiades, "A review of the melting curves of transition metals at high pressures using static compression techniques," *Crystals (Basel)*, vol. 11, no. 4, p. 416, Apr. 2021, doi: 10.3390/CRYST11040416/S1.

[14] D. R. Slocombe, V. L. Kuznetsov, W. Grochala, R. J. P. Williams, and P. P. Edwards, "Superconductivity in transition metals," *Philosophical Transactions of the Royal Society A: Mathematical, Physical and Engineering Sciences*, vol. 373, no. 2037, Mar. 2015, doi: 10.1098/RSTA.2014.0476.

[15] "Handbook of Refractory Carbides & Nitrides: Properties, Characteristics ... - Hugh O. Pierson - Google Books." https://books.google.ee/books?id=K_K7q3jaqXEC&pg=PA101&lpg=PA101&dq=All+these+properties+give+interstitial+carbides+great+importance+in+industrial+applications&source=bl&ots=Z0DFP3_xBo&sig=ACfU3U3Gp4mJvJeaT5gTqqhD_k5uy8qR2g&hl=en&sa=X&ved=2ahUKEwjo2NXKvKf3AhULgP0HHVM2CGUQ6AF6BAhEEAM#v=onepage&q=All%20these%20properties%20give%20interstitial%20carbides%20great%20importance%20in%20industrial%20applications&f=false (accessed Apr. 22, 2022).

[16] M. Sharma, M. Pathak, and P. N. Kapoor, "The sol-gel method: Pathway to ultrapure and homogeneous mixed metal oxide nanoparticles," *Asian Journal of Chemistry*, vol. 30, no. 7, pp. 1405–1412, 2018, doi: 10.14233/AJCHEM.2018.20845.

[17] “Synthesis and characterization of novel carbon electrodes for high power density electrochemical capacitors.” http://dspace.ut.ee/handle/10062/76845 (accessed Apr. 22, 2022).

[18] E. Yilmaz and M. Soylak, “Functionalized nanomaterials for sample preparation methods,” *Handbook of Nanomaterials in Analytical Chemistry: Modern Trends in Analysis*, pp. 375–413, Jan. 2019, doi: 10.1016/B978-0-12-816699-4.00015-3.

[19] S. Sakka and K. Kamiya, “The sol-gel transition in the hydrolysis of metal alkoxides in relation to the formation of glass fibers and films,” *Journal of Non-Crystalline Solids*, vol. 48, no. 1, pp. 31–46, Mar. 1982, doi: 10.1016/0022-3093(82)90244-7.

[20] M. Borlaf and R. Moreno, “Colloidal sol-gel: A powerful low-temperature aqueous synthesis route of nanosized powders and suspensions,” *Open Ceramics*, vol. 8, p. 100200, Dec. 2021, doi: 10.1016/J.OCERAM.2021.100200.

[21] “Hydrolysis of Metal Alkoxides and Synthesis of Simple Oxides by The Sol-Gel Method,” *The Chemistry of Metal Alkoxides*, pp. 107–125, Jan. 2002, doi: 10.1007/0-306-47657-6_9.

[22] S. Esposito, “‘Traditional’ Sol-Gel Chemistry as a Powerful Tool for the Preparation of Supported Metal and Metal Oxide Catalysts,” *Materials (Basel)*, vol. 12, no. 4, Feb. 2019, doi: 10.3390/MA12040668.

[23] S. Esposito, “‘Traditional’ sol-gel chemistry as a powerful tool for the preparation of supported metal and metal oxide catalysts,” *Materials*, vol. 12, no. 4, Feb. 2019, doi: 10.3390/MA12040668.

[24] V. Presser, M. Heon, and Y. Gogotsi, “Carbide-derived carbons - from porous networks to nanotubes and graphene,” *Advanced Functional Materials*, vol. 21, no. 5, pp. 810–833, Mar. 2011, doi: 10.1002/ADFM.201002094.

[25] “Carbon Allotropes: Metal-Complex Chemistry, Properties and Applications - Boris Ildusovich Kharisov, Oxana Vasilievna Kharissova - Google Books.” https://books.google.ee/books?id=O0OCDwAAQBAJ&pg=PA324&lpg=PA324&dq=The+structural+properties+of+CDC+can+be+from+porous+to+dense,+amorphous+to+crystal

line+and+from+sp2-+to+sp3-bonded.&source=bl&ots=WenUli-_gG&sig=ACfU3U32E_Rxr-DtRL5aERIKa9MER1JHuw&hl=en&sa=X&ved=2ahUKEwjQ_9Lpi_j2AhVd8rsIHUmZApsQ6AF6BAgCEAM#v=onepage&q=The%20structural%20properties%20of%20CDC%20can%20be%20from%20porous%20to%20dense%2C%20amorphous%20to%20crystalline%20and%20from%20sp2-%20to%20sp3-bonded.&f=false (accessed Apr. 03, 2022).

[26] R. K. Dash, G. Yushin, and Y. Gogotsi, "Synthesis, structure and porosity analysis of microporous and mesoporous carbon derived from zirconium carbide," *Microporous and Mesoporous Materials*, vol. 86, no. 1–3, pp. 50–57, Nov. 2005, doi: 10.1016/J.MICROMESO.2005.05.047.

[27] "Synthesis and characterization of new micro-mesoporous carbide derived carbon materials for high energy and power density electrical double layer capacitors." https://dspace.ut.ee/handle/10062/47593 (accessed May 22, 2022).

[28] Y. Fang, Q. Zhang, and L. Cui, "Recent progress of mesoporous materials for high performance supercapacitors," *Microporous and Mesoporous Materials*, vol. 314, p. 110870, Feb. 2021, doi: 10.1016/J.MICROMESO.2020.110870.

[29] V. Presser *et al.*, "Flexible Nano-felts of Carbide-Derived Carbon with Ultra-high Power Handling Capability," *Advanced Energy Materials*, vol. 1, no. 3, pp. 423–430, May 2011, doi: 10.1002/AENM.201100047.

[30] "Comparison between TiC-CDC-1000, ZrC-CDC-1000, and activated carbon.... | Download Scientific Diagram." https://www.researchgate.net/figure/Comparison-between-TiC-CDC-1000-ZrC-CDC-1000-and-activated-carbon-a-Volume-based_fig1_342614751 (accessed Apr. 03, 2022).

[31] M. R. Lukatskaya *et al.*, "Room-Temperature Carbide-Derived Carbon Synthesis by Electrochemical Etching of MAX Phases," *Angewandte Chemie International Edition*, vol. 53, no. 19, pp. 4877–4880, May 2014, doi: 10.1002/ANIE.201402513.

[32] E. N. Hoffman, G. Yushin, M. W. Barsoum, and Y. Gogotsi, "Synthesis of carbide-derived carbon by chlorination of Ti 2AlC," *Chemistry of Materials*, vol. 17, no. 9, pp.

2317–2322, May 2005, doi: 10.1021/CM047739I/ASSET/IMAGES/CM047739I.SOCIAL.JPEG_V03.

[33] B. A. J. Källén and E. Robert, “Drinking water chlorination and delivery outcome—a registry-based study in Sweden,” *Reproductive Toxicology*, vol. 14, no. 4, pp. 303–309, Jul. 2000, doi: 10.1016/S0890-6238(00)00086-1.

[34] “The structure and H2 diffusion in porous carbide-derived carbon particles.” https://dspace.ut.ee/handle/10062/76759 (accessed Apr. 22, 2022).

[35] A. Erdemir *et al.*, “Effects of high-temperature hydrogenation treatment on sliding friction and wear behavior of carbide-derived carbon films,” *Surface and Coatings Technology*, vol. 188–189, no. 1-3 SPEC.ISS., pp. 588–593, Nov. 2004, doi: 10.1016/J.SURFCOAT.2004.07.052.

[36] S. Yachamaneni *et al.*, “Mesoporous carbide-derived carbon for cytokine removal from blood plasma,” *Biomaterials*, vol. 31, no. 18, pp. 4789–4794, Jun. 2010, doi: 10.1016/J.BIOMATERIALS.2010.02.054.

[37] M. Oschatz, L. Borchardt, G. P. Hao, and S. Kaskel, “Nanoporous Carbide-Derived Carbons as Electrode Materials in Electrochemical Double-Layer Capacitors,” *Nanocarbons for Advanced Energy Storage*, vol. 1, pp. 417–453, Mar. 2015, doi: 10.1002/9783527680054.CH15.

[38] C. Pean *et al.*, “Confinement, Desolvation, and Electrosorption Effects on the Diffusion of Ions in Nanoporous Carbon Electrodes,” *J Am Chem Soc*, vol. 137, no. 39, pp. 12627–12632, Oct. 2015, doi: 10.1021/JACS.5B07416.

[39] X. Y. Tao, W. F. Qiu, H. Li, T. Zhao, and X. Y. Wei, “New route to synthesize preceramic polymers for zirconium carbide,” *Chinese Chemical Letters*, vol. 23, no. 9, pp. 1075–1078, Sep. 2012, doi: 10.1016/J.CCLET.2012.06.013.

[40] M. D. Sacks, C. A. Wang, Z. Yang, and A. Jain, “Carbothermal reduction synthesis of nanocrystalline zirconium carbide and hafnium carbide powders using solution-derived precursors,” *Journal of Materials Science 2004 39:19*, vol. 39, no. 19, pp. 6057–6066, Oct. 2004, doi: 10.1023/B:JMSC.0000041702.76858.A7.

[41] H. Preiss, E. Schierhorn, and K. W. Brzezinka, “Synthesis of polymeric titanium and zirconium precursors and preparation of carbide fibres and films,” *Journal of Materials Science 1998 33:19*, vol. 33, no. 19, pp. 4697–4706, 1998, doi: 10.1023/A:1004428818457.

[42] M. Inoue and I. Hirasawa, “The relationship between crystal morphology and XRD peak intensity on CaSO4·2H2O,” *Journal of Crystal Growth*, vol. 380, pp. 169–175, Oct. 2013, doi: 10.1016/J.JCRYSGRO.2013.06.017.

[43] R. S. Maurya and T. Laha, “The Glassy Structure Formation and Phase Evolution in Mechanically Alloyed and Spark Plasma-Sintered Al-TM-RE Alloys,” *Journal of Materials Engineering and Performance*, vol. 28, no. 12, pp. 7407–7418, Dec. 2019, doi: 10.1007/S11665-019-04505-1/FIGURES/10.

[44] H. Kurig, M. Russina, I. Tallo, M. Siebenbürger, T. Romann, and E. Lust, “The suitability of infinite slit-shaped pore model to describe the pores in highly porous carbon materials,” *Carbon N Y*, vol. 100, pp. 617–624, Apr. 2016, doi: 10.1016/J.CARBON.2016.01.061.

[45] F. Stoeckli and T. A. Centeno, “On the determination of surface areas in activated carbons,” *Carbon N Y*, vol. 43, no. 6, pp. 1184–1190, 2005, doi: 10.1016/J.CARBON.2004.12.010.

[46] M. Q. Xue, H. Tang, and C. S. Li, “Synthesis and tribological properties of TiC micro and nanoparticles,” *International Journal of Surface Science and Engineering*, vol. 9, no. 1, pp. 69–80, Jan. 2015, doi: 10.1504/IJSURFSE.2015.067040.

To the vice dean for academic affairs of the Faculty of Science and Technology, University of Tartu

Application for establishing restrictions on the publishing of the graduation thesis, and declaring the defence private

Name	Selin Su Yegit
Date of birth	08.07.2001
Curriculum	Science and techology
Supervisor	Maarja Paalo
Graduation thesis title	Synthesis of zirconium carbide derived carbon using sol-gel method, carbothermal reduction and chlorination

[X] I request my graduation thesis not to be published until 31.12.2022 (date) for the reason indicated below:

- [ ] Economic copyright rights belong to other people
- [ ] Thesis includes personal data and the data subject has not agreed to publishing
- [ ] State secret
- [ ] Trade secret
- [X] In future, the graduation thesis will be published as a scientific article
- [ ] Other reasons

Explanation (reasons why restrictions are applied for and why for the particular period):

☐ I request my defence to be declared private.

Explanation (reasons for declaring the defence private):

Application has the following annexes (to be filled in if there are annexes, i.e. the company's confirmation that the thesis involves a trade secret):

1.
2.

Date and student's signature _____

Date and supervisor's signature _____